

The N–H···S Hydrogen Bond in (TACN)₂Fe₂S₆ (TACN = Triazacyclononane) and in Model Systems Involving the Persulfido Moiety: An ab Initio and DFT Study

Stéphane François,[†] Marie-Madeleine Rohmer,[†] Marc Bénard,^{*,†}
Andrew C. Moreland,[‡] and Thomas B. Rauchfuss[‡]

Contribution from the Laboratoire de Chimie Quantique, UMR 7551, CNRS and Université Louis Pasteur, F-67000 Strasbourg, France, and School of Chemical Sciences, University of Illinois, Urbana, Illinois 61801

Received April 3, 2000. Revised Manuscript Received October 11, 2000

Abstract: Extended Hückel, DFT, and ab initio MP2 calculations have been carried out to rationalize the unprecedented structural characteristics of the recently synthesized complex $(\mu-\eta^1-S_2)_3(Fe-TACN)_2$ (TACN = triazacyclononane). The orbital interaction diagram between the metal–macrocycle dimer and the three disulfide ligands accounts for some of the observed properties of the complex: diamagnetism, existence of an Fe–Fe single bond, nucleophilicity of the terminal sulfur atoms. The unprecedented occurrence of a M₂S₆ core, as the very unusual $\mu-\eta^1$ coordination of the S₂ ligands, however, requires further analysis. It was assumed that the key to the structural singularities of this complex should be sought in the network of intramolecular H···S bonds revealed by the crystallographic analysis and involving all six NH groups and all three terminal S atoms. We therefore report the first quantitative theoretical investigation of the energetics of intramolecular H···S bonds. Geometry optimizations have been carried out by means of the Density Functional Theory (DFT) on two configurations of $(\mu-\eta^1-S_2)_3(Fe-TACN)_2$ deduced one from another by inverting the pyramidalities at the proximal sulfur atoms. The experimental conformation **1**, characterized by six “strong” N–H···S bonds ($d_{H\dots S} = 2.31 \text{ \AA}$), is more stable by 10.0 kcal·mol⁻¹ than the hypothetical structure **2** with “weak” hydrogen bonds ($d_{H\dots S} = 2.65 \text{ \AA}$). Replacing persulfide by sulfoxide ligands leads to a similar energy difference (11.4 kcal·mol⁻¹), despite the well-documented tendency to obtain stronger H bonds with oxygen than with sulfur. Those results are rationalized by means of a systematic investigation, at the DFT and MP2 levels, of the N–H···S and N–H···O interactions in the model systems C₂H₄SX···HNH₂ (X = S, O). The strength of the N–H···X interaction is shown to be highly dependent on the directionality of the hydrogen bond characterized by the angle $\theta = H-X-S$. For X = S, the optimal interaction is obtained for $\theta \sim 80^\circ$, which almost exactly reproduces the angular parameter optimized in **1** (76.7°). For X = O, the interaction is most favorable for higher values of θ (~115°) which cannot be obtained in the hypothetical compound $(\mu-\eta^1-SO)_3(Fe-TACN)_2$ because of structural constraints. Finally, varying the H···X distance in the models shows that those interactions are extremely far-reaching. The energy difference between conformations **1** and **2** then accounts for only a small part of the global stabilization assigned to the hydrogen bond network, which could hence represent the key to the stabilization of the Fe₂S₆ core.

1. Introduction

Ab initio calculations^{1–5} and a statistical treatment of the crystallographic data recently retrieved from the Cambridge Structural Database^{5,6} indicate that the hydrogen-bonding ability of sulfur, in its terminal (X = S), divalent (Y–S–Z), or negatively charged (R–S⁻) states, is weaker than that of oxygen in a similar environment. The importance of intramolecular

N–H···S hydrogen bonds involving thiolate ligands has, however, been recognized for more than 20 years in mono- and polymetallic iron–sulfur proteins,^{7–9} and in related complexes of cobalt¹⁰ and molybdenum.¹¹ More recently, the presence of single or double N–H···S hydrogen bonds was suggested in

(7) (a) Carter, C. W., Jr. *J. Biol. Chem.* **1977**, *252*, 7802. (b) Sheridan, R. P.; Allen, L. C.; Carter, C. W., Jr. *J. Biol. Chem.* **1981**, *256*, 5052.

(8) Doan, P. E.; Fan, C.; Hoffman, B. M. *J. Am. Chem. Soc.* **1994**, *116*, 1033.

(9) (a) Ueyama, N.; Terakawa, T.; Nakata, M.; Nakamura, A. *J. Am. Chem. Soc.* **1983**, *105*, 7098. (b) Ueyama, N.; Kajiwara, A.; Terakawa, T.; Ueno, T.; Nakamura, A. *Inorg. Chem.* **1985**, *24*, 4700. (c) Ohno, R.; Ueyama, N.; Nakamura, A. *Inorg. Chem.* **1991**, *30*, 4887. (d) Sun, W.-Y.; Ueyama, N.; Nakamura, A. *Inorg. Chem.* **1991**, *30*, 4026.

(10) (a) Walters, M. A.; Dewan, J. C.; Min, C.; Pinto, S. *Inorg. Chem.* **1991**, *30*, 2656. (b) Okamura, T.; Takamizawa, S.; Ueyama, N.; Nakamura, A. *Inorg. Chem.* **1998**, *37*, 18.

(11) (a) Ueyama, N.; Okamura, T.; Nakamura, A. *J. Am. Chem. Soc.* **1992**, *114*, 8129. (b) Huang, J.; Walters, M. A. *J. Inorg. Biochem.* **1993**, *51*, 24. (c) Ueyama, N.; Yoshinaga, N.; Kajiwara, A.; Nakamura, A. *Chem. Lett.* **1990**, *117*, 1781. (d) Huang, J.; Ostrander, R. L.; Rheingold, A. L.; Leung, Y.; Walters, M. A. *J. Am. Chem. Soc.* **1994**, *116*, 6769.

[†] CNRS and Université Louis Pasteur.

[‡] University of Illinois.

(1) Sennikov, P. G. *J. Phys. Chem.* **1994**, *98*, 4973.

(2) Frisch, M. J.; Pople, J. A.; Del Bene, J. A. *J. Phys. Chem.* **1985**, *89*, 3664.

(3) (a) Vibok, A.; Mayer, I. *Int. J. Quantum Chem.* **1992**, *43*, 801. (b) Valiron, P.; Vibok, A.; Mayer, I. *J. Comput. Chem.* **1993**, *14*, 401. (c) Vibok, A.; Halasz, G.; Mayer, I. *Mol. Phys.* **1998**, *93*, 873.

(4) Zheng, Y.-J.; Merz, K. M., Jr. *J. Comput. Chem.* **1992**, *13*, 1151.

(5) Platts, J. A.; Howard, S. T.; Bracke, B. R. F. *J. Am. Chem. Soc.* **1996**, *118*, 2726.

(6) Allen, F. H.; Bird, C. M.; Rowland, R. S.; Raithby, P. R. *Acta Crystallogr.* **1997**, *B53*, 680; 696.

the active site of various cytochrome P450s¹² and characterized in their synthetic models.^{13,14} The role of those hydrogen bonds seems to be crucial in stabilizing the Fe(III) state and protecting the complex against decomposition.¹³ The influence of the N–H···S interactions in the regulation of the redox potential of the metal–sulfur proteins and other complexes is particularly well-documented^{7,9,11a,15} and could prevent water-induced dissociation of the M–S bond under neutral conditions.¹⁶ The coordination of N₂H₂ to two iron–tetrathiolate centers in a complex proposed to be a model for enzymatic N₂ fixation was shown to be stabilized through strong N–H···S hydrogen bonds.¹⁷ Few theoretical studies have been performed on those complexes. Ab initio calculations have, however, been reported in which the N–H···S interaction in (Cys-S)₄Fe₄S₄ clusters is modeled by formamide-SHX and formamide-SX₃ hydrogen-bonded complexes where X is a pseudoatom with a variable nuclear charge.^{7b} Extended Hückel calculations have been carried out on a model of the [Mo^VO(S-*o*-CH₃CONHC₆H₄)₄][−] complex.^{11a} The conformations of the thiolate ligand compatible with a hydrogen bond in that cluster were inferred from the variation of the N–H···S overlap population with change of the S–C torsional angle. No study focused on the energetics of those hydrogen bonds in situ has, however, been reported to date, probably because of the intramolecular character of the interactions, which precludes the design of a reference conformation *without* the N–H···S bond.

The recent synthesis and X-ray characterization of a dimer of Fe^{III}triazacyclononane (TACN) bridged with three persulfido ligands¹⁸ (Figure 1a,b) provides an opportunity to investigate the intramolecular N–H···S interaction and its energetic contribution to the stabilization of that unprecedented M₂(S₂)₃ core. The goal of this work is to report DFT and ab initio MP2 calculations carried out on that complex in two conformations. Those conformations, represented in Figure 1b,c, are equivalent as far as orbital interactions are concerned and only differ in the strength of the N–H···S bond network connecting the six NH groups to the three terminal S atoms. The hypothetical complex in which the persulfido ligands are replaced by sulfoxide moieties is also investigated. The information obtained on the energetics of those N–H···S and N–H···O interactions will be completed by a description of the approach of one or two NH₃ molecules to C₂H₄(S₂) and C₂H₄(SO) model systems.

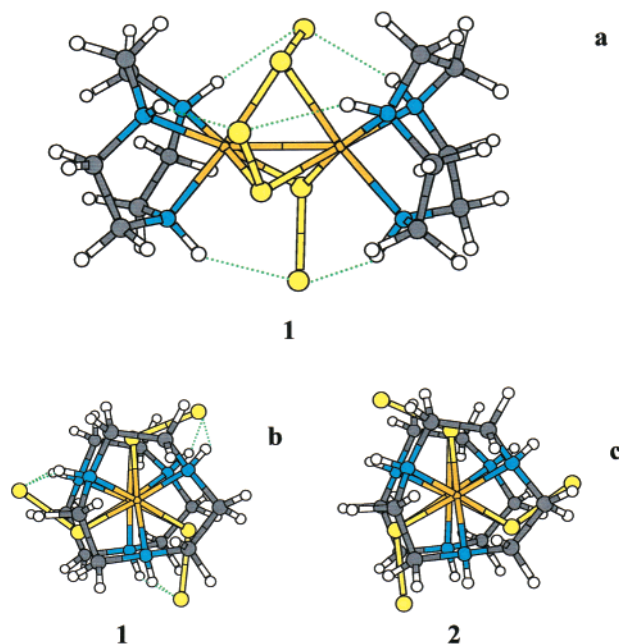


Figure 1. (a and b) Two X-ray representations of $(\mu\text{-S}_2)_3(\text{Fe-TACN})_2$ in conformation **1**, corresponding to the experimental structure, with a network of “strong” N–H···S bonds and (c) X-ray representation of conformation **2**, derived from **1** by inverting the pyramidality of the proximal sulfur atoms.

2. Computational Details

Calculations on both conformations of $(\mu\text{-SX})_3(\text{Fe-TACN})_2$ (X = S, O) (Figure 1) as well as on the model systems have been carried out with the ADF program.¹⁹ The formalism is based upon the local spin density approximation characterized by the electron gas exchange ($X\alpha$ with $\alpha = 2/3$) together with Vosko–Wilk–Nusair²⁰ parametrization for correlation. Nonlocal corrections due to Becke for the exchange energy²¹ and to Perdew for the correlation energy²² have been added. For first-row atoms, a 1s frozen core was described by means of a single Slater function. For iron and sulfur, the frozen core composed of the 1s and 2sp shells was also modeled by a minimal Slater basis. For all atom types except for iron, the Slater basis set used for the valence shell is of triple- ζ quality and completed by a p- or d-type polarization function.²³ The 3s and 3p shells of iron are described by a double- ζ Slater basis, the 3d and 4s shells by a triple- ζ basis, and the 4p shell by a single orbital. No f-type polarization function is added. The geometry optimization processes have been carried out by minimizing the energy gradient by the BFGS formalism²⁴ combined with a DIIS-type convergence acceleration method.²⁵ The optimization cycles were continued until all of the three following convergence criteria were fulfilled: (i) the difference in the *total energy* between two successive cycles is less than 0.001 hartree; (ii) the difference in the *norm of the gradient* between two successive cycles is less than 0.01 hartree·Å^{−1}; and (iii) the maximal difference in the *Cartesian*

(12) (a) Poulos, T. L.; Finzel, B. C.; Howard, A. J. *J. Mol. Biol.* **1987**, *195*, 687. (b) Sundaramoorthy, M.; Ternier, J.; Poulos, T. L. *Structure* **1995**, *3*, 1367. (c) Li, H.; Poulos, T. L. *Acta Crystallogr.* **1995**, *D51*, 21. (d) Hasemann, C. A.; Ravichandran, K. G.; Peterson, J. A.; Deisenhofer, J. *J. Mol. Biol.* **1994**, *236*, 1169. (e) Cupp-Vickery, J. R.; Poulos, T. L. *Nature Struct. Biol.* **1995**, *2*, 144. (f) Crane, B. R.; Arvai, A. S.; Gachhui, R.; Wu, C.; Ghosh, D. K.; Getzoff, E. D.; Stuehr, D. J.; Tainer, J. A. *Science* **1997**, *278*, 425.

(13) (a) Ueyama, N.; Nishikawa, N.; Yamada, Y.; Okamura, T.; Nakamura, A. *J. Am. Chem. Soc.* **1996**, *118*, 12826. (b) Ueno, T.; Nishikawa, N.; Moriyama, S.; Adachi, S.; Lee, K.; Okamura, T.; Ueyama, N.; Nakamura, A. *Inorg. Chem.* **1999**, *38*, 1199. (c) Ueno, T.; Kousumi, Y.; Yoshizawa-Kumagaya, K.; Nakajima, K.; Ueyama, N.; Okamura, T.; Nakamura, A. *J. Am. Chem. Soc.* **1998**, *120*, 12264. (d) Suzuki, N.; Higuchi, T.; Urano, Y.; Kikuchi, K.; Uekusa, H.; Ohashi, Y.; Uchida, T.; Kitagawa, T.; Nagano, T. *J. Am. Chem. Soc.* **1999**, *121*, 11571.

(14) Ueyama, N.; Nishikawa, N.; Yamada, Y.; Okamura, T.; Oka, S.; Sakurai, H.; Nakamura, A. *Inorg. Chem.* **1998**, *37*, 2415.

(15) (a) Ueno, T.; Ueyama, N.; Nakamura, A. *J. Chem. Soc., Dalton Trans.* **1996**, 3859. (b) Huang, J.; Ostrander, R. L.; Rheingold, A. L.; Walters, M. A. *Inorg. Chem.* **1995**, *34*, 1090.

(16) Ueyama, L.; Inohara, M.; Onoda, A.; Ueno, T.; Okamura, T.; Nakamura, A. *Inorg. Chem.* **1999**, *38*, 4028.

(17) (a) Sellmann, D.; Soglowek, W.; Knoch, F.; Moll, M. *Angew. Chem., Int. Ed. Engl.* **1989**, *28*, 1271. (b) Sellmann, D. *New J. Chem.* **1997**, *21*, 681.

(18) Moreland, A. C.; Rauchfuss, T. B. *J. Am. Chem. Soc.* **1998**, *120*, 9376.

(19) (a) *ADF 2.3 User's Guide*; Chemistry Department, Vrije Universiteit: Amsterdam, The Netherlands, 1997. (b) Baerends, E. J.; Ellis, D. E.; Ros, P. *Chem. Phys.* **1973**, *2*, 41. (c) te Velde, G.; Baerends, E. J. *J. Comput. Phys.* **1992**, *99*, 84. (d) Fonseca-Guerra, C.; Visser, O.; Snijders, J. G.; te Velde, G.; Baerends, E. J. *Methods and Techniques in Computational Chemistry: METECC-95*; Clementi, E., Corongiu, G., Eds.; STEF: Cagliari, Italy, 1995; pp 305–395.

(20) Vosko, S. H.; Wilk, L.; Nusair, M. *Can. J. Phys.* **1980**, *58*, 1200.

(21) (a) Becke, A. D. *J. Chem. Phys.* **1986**, *84*, 4524. (b) Becke, A. D. *Phys. Rev.* **1988**, *A38*, 3098.

(22) Perdew, J. P. *Phys. Rev.* **1986**, *B33*, 8882; *B34*, 7406.

(23) Snijders, J. G.; Baerends, E. J.; Vernooijs, P. *At. Nucl. Tables* **1982**, *26*, 483. (b) Vernooijs, P.; Snijders, J. G.; Baerends, E. J. *Slater type basis functions for the whole periodic system*; Internal Report, Free University of Amsterdam: Amsterdam, The Netherlands, 1981.

(24) Fisher, T. H.; Almlöf, J. *J. Phys. Chem.* **1992**, *96*, 9768.

(25) Versluis, L. Ph.D. Thesis, University of Calgary, Calgary, Alberta, Canada, 1989.

coordinates between two successive cycles is less than 0.01 Å. The Gaussian 98 package²⁶ has then been used to carry out single point calculations at the ab initio MP2 level on the diiron complexes, using the optimal geometries obtained from ADF. 6-31G basis sets were used for that calculation, except for the atoms of the Fe₂S₆ core and the H atoms involved in the hydrogen bond, for which the basis set was completed by a polarization function. The complete modelization of the approach of one or two NH₃ molecules to (C₂H₄)S₂ and (C₂H₄)SO, carried out first with ADF, has been replicated at the ab initio MP2 level. The LANL2DZ basis sets, augmented with one polarization function for all atoms, were preferred in that study to the 6-31G* basis sets, to reduce the influence of the basis set superposition error (BSSE). The interaction energies calculated for the model systems were eventually corrected from BSSE by means of the counterpoise method of Boys and Bernardi.²⁷

3. Electronic Structure of Fe₂S₆(TACN)₂

The complex synthesized at the University of Illinois belongs to the family of faced-shared bioctahedra, where each Fe atom is bound in an N₃S₃ coordination sphere. The bonding in those complexes has been discussed in terms of structural distortions by Cotton and Ucko,²⁸ and analyzed by means of extended Hückel calculations by Summerville and Hoffmann.²⁹ According to Cotton and Ucko, the presence of a metal–metal bond in such complexes cannot be deduced from the sole value of the metal–metal distance, due to the limited flexibility of the bridge system. They rather advocate structural criteria that measure the deformation of the molecular framework with respect to a perfect bioctahedron, such as β , the angle at the bridging group, and α , the angle between any two ligands on the same metal. α and β are expected to be 90° and 70.5°, respectively, in an ideal M₂L₉ structure. In the crystal structure of Fe₂S₆(TACN)₂, the S–Fe–S α angles are very slightly above 90° and the β angles at the bridging sulfur are also close to the borderline, with values between 69° and 71°. Therefore, despite the short Fe–Fe distance (2.546 Å), no clear structural indication is provided in favor of a strong metal–metal bond. A single metal–metal coupling is, however, required to complete to 18 electrons the environment of each Fe atom and to account for the observed diamagnetism.

The main orbital interactions that occur in triply bridged dimers with π -donating bridging ligands, exemplified by (Cl)₃, have been schematized by Summerville and Hoffmann.²⁹ The substitution of chlorine with disulfide (S₂)²⁻ as bridging ligands, however, makes the orbital interaction diagram slightly more complex. The main interactions involving the frontier orbitals of the Fe(TACN) dimer and the (S₂)₃ fragment have therefore been summarized in Figure 2. For the sake of simplicity, interactions involving orbitals respectively antisymmetric (A'' representation) and symmetric (A' representation) with respect to the symmetry plane containing the disulfide ligands have been represented separately.

(26) Gaussian 98, Revision A.5; Frisch, M. J.; Trucks, G. W.; Schlegel, H. B.; Scuseria, G. E.; Robb, M. A.; Cheeseman, J. R.; Zakrzewski, V. G.; Montgomery, J. A., Jr.; Stratmann, R. E.; Burant, J. C.; Dapprich, S.; Millam, J. M.; Daniels, A. D.; Kudin, K. N.; Strain, M. C.; Farkas, O.; Tomasi, J.; Barone, V.; Cossi, M.; Cammi, R.; Mennucci, B.; Pomelli, C.; Adamo, C.; Clifford, S.; Ochterski, J.; Petersson, G. A.; Ayala, P. Y.; Cui, Q.; Morokuma, K.; Malick, D. K.; Rabuck, A. D.; Raghavachari, K.; Foresman, J. B.; Cioslowski, J.; Ortiz, J. V.; Stefanov, B. B.; Liu, G.; Liashenko, A.; Piskorz, P.; Komaromi, I.; Gomperts, R.; Martin, R. L.; Fox, D. J.; Keith, T.; Al-Laham, M. A.; Peng, C. Y.; Nanayakkara, A.; Gonzalez, C.; Challacombe, M.; Gill, P. M. W.; Johnson, B.; Chen, W.; Wong, M. W.; Andres, J. L.; Gonzalez, C.; Head-Gordon, M.; Replogle, E. S.; Pople, J. A. Gaussian, Inc.: Pittsburgh, PA, 1998.

(27) Boys, S. F.; Bernardi, F. *Mol. Phys.* **1970**, *19*, 553.

(28) Cotton, F. A.; Ucko, D. A. *Inorg. Chim. Acta* **1972**, *6*, 161.

(29) Summerville, R. H.; Hoffmann, R. *J. Am. Chem. Soc.* **1979**, *101*, 3821.

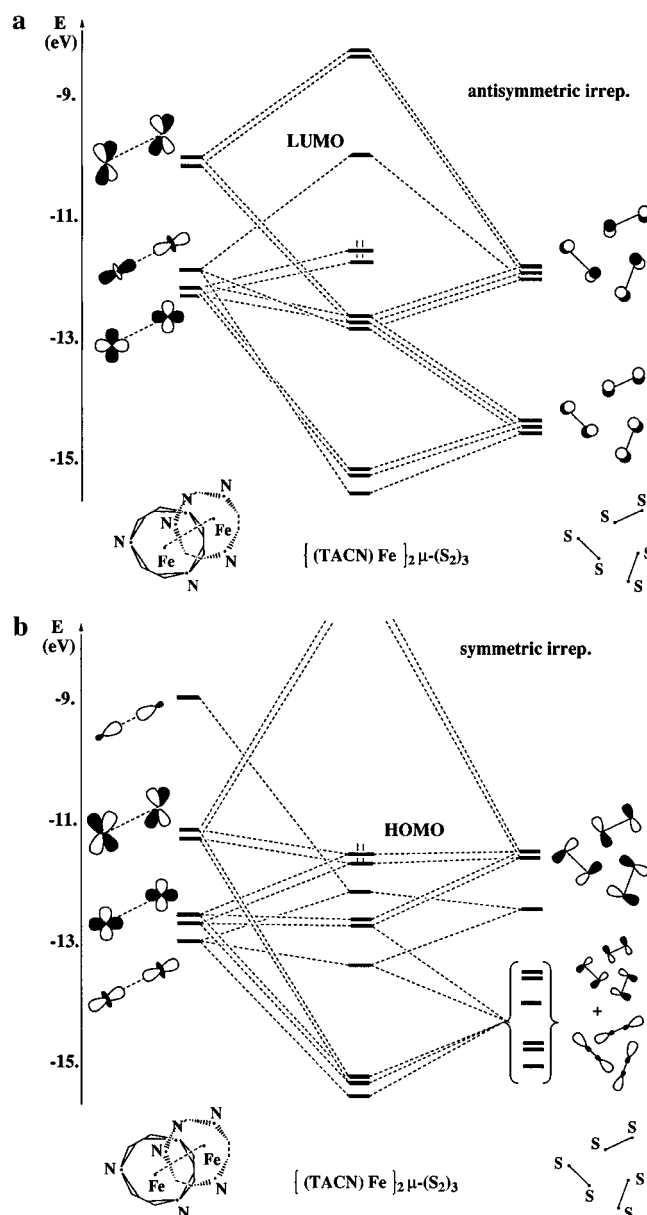


Figure 2. Orbital interaction diagram between the Fe-TACN dimer and three disulfide fragments, from extended Hückel calculations: (a) orbitals antisymmetric with respect to the plane containing the three disulfides and (b) orbitals symmetric with respect to that plane.

The orbitals of the ML₃ fragment are well-known.³⁰ The three orbitals of the t_{2g} set are pure metal orbitals, unaffected by coordination. Higher in energy, the e_g orbitals are destabilized through σ -donation. In the ML₃ dimer, each of those orbitals gives rise to two combinations, one symmetric and one antisymmetric with respect to the symmetry plane. The degeneracy of the t_{2g} set is broken by the σ interaction between the d_{z²} orbitals, giving rise to a metal–metal bonding level with a' symmetry (−12.8 eV), and to its antibonding counterpart in the other representation (−11.8 eV). A high energy level (−8.8 eV) with s-bonding character arises in the A' representation. Assuming a formal charge of 6+ for the dimer, the orbitals of the t_{2g} combinations are populated with 10 electrons altogether, and those of the e_g sets are empty (Figure 2).

Each disulfide unit, formally 2−, has one π and one π^* orbital, both occupied, with a'' symmetry. The interactions

(30) Albright, T. A.; Burdett, J. K.; Whangbo, M. H. *Orbital Interactions in Chemistry*; Wiley-Interscience: New York, 1985.

Table 1. Structural Parameters Obtained for $(\mu\text{-SX})_3(\text{Fe-TACN})_2$ from DFT Gradient Optimization (Conformations **1** and **2**, X = S, O) and from X-ray Diffraction (Conformation **1**, X = S) and Relative Energies (ΔE , kcal·mol⁻¹) for Conformations **1** and **2** at the DFT and MP2 Levels^a

structural parameter	X = S			X = O	
	1 (exptl)	1 (calcd)	2 (calcd)	1 (calcd)	2 (calcd)
Fe–Fe	2.55	2.53	2.55	2.47	2.48
Fe–S	2.19–2.26	2.25	2.25	2.21	2.19
S–X	1.97–2.11	2.11	2.10	1.62	1.59
Fe–N	1.99–2.07	2.07	2.08	2.09	2.09
C–N	1.45–1.52	1.48–1.50	1.48–1.50	1.48–1.49	1.48–1.49
C–C	1.48–1.53	1.535	1.533	1.539	1.540
N–H	0.76–1.14	1.046	1.036	1.034	1.030
H···X	2.40–2.62	2.31–2.32	2.635–2.66	2.19–2.21	2.68–2.69
S–X–Fe	107.1–113.8	109.2	111.0	109.7	112.0
Fe–S–Fe	68.8–70.7	68.4	69.1	67.9	69.0
pyramidalicity at S_{prox}^b	288.0–293.9	286.8	291.1	287.3	293.0
H–X–S		76.7	76.9	88.2	89.3
rel energies					
ΔE (DFT)		0.0	+10.0	0.0	+11.4
ΔE (MP2)		0.0	+16.2	0.0	+7.2

^a Bonding energies (DFT) and total energies (MP2) are provided as Supporting Information. ^b Measured by the sum of the three angles at the proximal sulfur.

between the three ligands are negligible in that representation, and the antisymmetric combinations of the S_2 trimer remain clustered around -14.4 eV for the π levels, and -11.9 eV for the π^* levels. Similar combinations of π and π^* orbitals occur in the symmetry plane, but a splitting of ~ 1 eV affects both clusters of levels. Moreover, the π level of S_2 is accidentally degenerate with the lone pair orbital, which gives rise for $(S_2)_3$ in the symmetric representation to a cluster of six intermingled orbitals between -13.5 and -15.0 eV (Figure 2).

The most important interactions in the antisymmetric representation affect the σ -antibonding orbital of the Fe-TACN dimer and the e_g -type levels with higher energy (Figure 2a). Each of those orbitals simultaneously interacts with two appropriately suited combinations of the bridging fragments, one with π character, the other with π^* character. Each of those three-term interactions gives rise to three levels in the resulting complex: a low-energy level (-15.1 to -15.6 eV) with metal–sulfur bonding character; an intermediate level (-12.6 to -12.8 eV) with nonbonding character; and a destabilized, antibonding level. One of these high-energy levels, also displaying metal–metal σ -antibonding character, represents the LUMO, at -9.9 eV. It is interesting to note that the nonbonding Fe–S character of the intermediate cluster of levels is obtained through a transfer of the electron density from the proximal to the terminal sulfur atom in the S_2 fragments. By contrast, the density in the high-lying, unoccupied levels is concentrated in the proximal sulfur atoms. Then, the three-term interactions involving the π and π^* levels of S_2 on the one side and the appropriate dimetal combinations on the other side account for the nucleophilicity of the terminal sulfur atoms postulated in a preliminary account.¹⁸ The two remaining orbitals of the t_{2g} set are also somewhat reorganized by the insertion of some e_g character, but they remain largely dimetallic (76%) at -11.7 eV.

The orbital interactions in the symmetric representation are qualitatively similar, but the in-phase metal orbitals of the e_g set are in better position to overlap with the π^* combinations of the disulfide fragments. As a result, the antibonding MOs are rejected higher in energy, whereas the intermediate levels retain an important bonding character with the proximal sulfur atoms. These quasidegenerate levels give rise to the HOMO, at -11.5 eV (Figure 2b). The metal–metal σ -bonding orbital is split into three components, respectively antibonding (-12.1 eV), nonbonding (-13.1), and bonding (-15.4) with respect

Table 2. Atomic and Fragment Charges (e) Obtained from Mulliken Population Analyses Carried Out on the Extended Hückel (EHT), the DFT, and the Ab Initio Wave Functions of $(\mu\text{-SX})_3(\text{Fe-TACN})_2$ (X = S, O)

	EHT		DFT		ab initio	
	X = S	X = O	X = S	X = O	X = S	X = O
S	+0.30	+0.75	-0.03	+0.12	-0.42	+0.13
X	-0.91	-1.40	-0.57	-0.65	-0.49	-0.86
Fe	-0.31	-0.29	+0.71	+0.60	+1.13	+0.82
$(SX)_3$	-1.83	-1.95	-1.80	-1.60	-2.73	-2.19
TACN	+1.23	+1.27	+0.18	+0.20	+0.23	+0.27

to $(S_2)_3$. All three levels are doubly occupied and contribute to the metal–metal single bond in the complex. As in the antisymmetric representation, the two Fe– (S_2) nonbonding levels originating in the t_{2g} set (-12.6 eV) display important weight on the terminal sulfur atoms. A Mulliken population analysis of the EHT wave function yields point charges of $-0.3e$ on Fe, $+0.3e$ on proximal S atoms, and $-0.9e$ on terminal sulfurs. It is important to note that the negative charge on terminal sulfurs almost exclusively originates in the π orbitals, perpendicular to the S–S axis. Both π systems are equally contributing, so that the charge density is uniformly distributed around the terminal S atoms, as will be discussed further about the model systems. This means that the donation interactions from the $(S_2)^{2-}$ ligands to the metal involve the proximal sulfurs without too much contribution from the terminal atoms, except for some charge transfer through the orbitals oriented along the S–S axis. Another practical consequence concerns the orientation most probable for a hydrogen bond, since the incoming H atom will preferably approach the terminal sulfur in the direction of the π orbitals, that is approximately *perpendicular* to the S–S bond.

Extended Hückel calculations tend to overemphasize the importance of density transfers. Despite this systematic bias, the Mulliken analyses carried out from EHT, DFT, and ab initio calculations (Table 2) agree on the fact that the disulfide ligands retain an important part of their formal negative charge, mainly localized in the terminal sulfurs as noted above. Density donation from the macrocycles and from the disulfides overcompensates (with EHT) or partly compensates (with DFT and MP2) the formal positive charge of Fe(III). Finally, the plane of the S_2 trimer represents a strongly nucleophilic region acting as an electrostatic attractor toward positively charged TACN

macrocycles (Table 2). The low electrostatic potential generated by the (S₂)₃ ligands in the symmetry plane could explain the specific strength of the N–H···S hydrogen bond network in (μ–S₂)₃(Fe–TACN)₂.

4. Geometry Optimizations: Technique and Results

A complete optimization of the geometry of (μ–S₂)₃(Fe–TACN)₂ was carried out, starting from the X-ray structure. The most significant structural parameters of the optimized structure, referred to as conformation **1**, are displayed in Table 1, and compared to experiment. Although the only constraints imposed on the optimization process were those of the symmetry plane containing the disulfide ligands, the geometry obtained at convergence corresponds to the C_{3v} symmetry, at the precision of gradient optimization. The differences observed in the crystal structure between parameters that should be equivalent in a cluster with 3-fold symmetry, and particularly between the three S–S distances (1.97, 2.04, and 2.11 Å),¹⁸ should therefore be assigned to the effect of crystal packing. The optimized distances are in the range of the observed parameters, although they tend to be slightly above the average values. There is, however, an important exception concerning the H···S contacts, which are found considerably shorter in the calculated structure (2.31–2.32 Å) than in the experimental one (2.40–2.62 Å). This should be assigned to the combination of several effects. First, the position of the hydrogen atoms determined by X-ray diffraction is extremely inaccurate and affected by a systematic bias which reduces the observed length of the CH, NH, or OH bonds.³¹ In the present structure, the average value of the NH bond lengths deduced from the observed hydrogen positions is 0.93 Å, compared to an experimental determination of 1.012 Å in NH₃, and to a value of 1.046 Å calculated for complex **1** (Table 1). Assigning to the N–H bond length a value of 1.046 Å reduces the average length of the H···S contacts by about 0.1 Å, which is not sufficient to account for the difference between the observed and the calculated values. The rest of the gap, which is close to 0.1 Å, is explained by a slightly more pronounced pyramidal character of the proximal sulfur atoms in the calculated structure of **1**. The sum of the angles at these S atoms is computed to be 286.8°, compared to an average value of 291.6° in the crystal structure.³²

Then, a second conformation was defined from the optimal structure of **1**. Conformation **2** is deduced from **1** by making each terminal S atom undergo a reflection with respect to the plane defined by the two Fe atoms and the proximal sulfur (Figure 1c).³³ This yields an inversion of the pyramidal character of the proximal sulfurs, with no change either in the coordination sphere of the Fe atoms or even in most geometrical parameters, *except for an important stretching of the NH···S hydrogen bonds, from 2.31 to 2.65 Å*. One can therefore infer that the energy differences obtained at the DFT or MP2 levels between structures **1** and **2** will be exclusively related to the changes in the hydrogen bonding network.

Further geometry optimization carried out on **2** with the H···S distances constrained to remain fixed at 2.65 Å only yielded

small modifications in the structure of the coordination sphere, all of which can be interpreted as consequences of the weakening of the NH···S hydrogen bonds (Table 1). The most significant examples are the shortening of the N–H bond length, from 1.046 to 1.036 Å, and the reduction of the pyramidal character of the proximal sulfur atoms, measured by the greater sum of the three bond angles at these atoms (291.1°, compared to 286.8° in **1**). The slight increase of the Fe–Fe bond length itself, from 2.53 to 2.55 Å, can be seen as a response of the cluster core to the relaxation occurring in the most external part of the ligand sphere. A full description of the geometry optimized for **1** and **2** is provided as Supporting Information.

The energy difference obtained at the DFT level between the optimized structures of **1** and **2** is 10.0 kcal·mol^{−1} in favor of **1** (Table 1), which corresponds to about 1.7 kcal·mol^{−1} for each NH···S interaction. This value should, however, be interpreted with caution, since it is expected for several reasons to represent a *lower bound* to the exact interaction energy in the complex. As a matter of fact, the H···S distances in **2** (2.65 Å) are still short enough to infer the existence of residual interactions. Another open question concerns the additivity of two NH···S interactions pointing toward the same sulfur atom. These points will be discussed in relation to the model systems (Section 5). Finally, the DFT formalism is not supposed to provide a full account of the energy involved in nonbonded interactions: although the electrostatic effects are adequately described, the dispersion forces are either ignored³⁴ or at least imperfectly accounted for.³⁵ Ab initio calculations at the MP2 level have been shown to provide a more reliable account for those effects.³⁴ As a matter of fact, the energy difference between **1** and **2** calculated at the MP2 level with the geometries optimized with DFT amounts to 16 kcal·mol^{−1}, which corresponds to a difference of 2.7 kcal·mol^{−1} between a “strong” NH···S bond as in **1** and a “sensibly weaker” NH···S bond as in **2**.

Geometry optimizations at the DFT and MP2 levels of calculation have been carried out according to the same procedure in the hypothetical complexes in which the disulfide has been replaced by sulfoxide ligands (see Supporting Information). Rather surprisingly, the H···O distances optimized in conformation **1** (2.19–2.21 Å) are not exceedingly shorter than the H···S distances calculated for the disulfido complex (2.31–2.32 Å). However, the structural differences obtained between conformations **1** and **2**, and particularly the change in the pyramidal character at S_{prox}, are similar to those obtained for (μ–S₂)₃–(Fe–TACN)₂ and suggest the existence of a hydrogen bond network significantly stronger in **1** than in **2**. The calculated energy differences in favor of conformation **1**, 11.4 kcal·mol^{−1} with DFT and 7.2 kcal·mol^{−1} with MP2 (Table 1), confirm that such a network could exist in a hypothetical sulfoxide complex. In view of the comparisons reported in the literature between the relative strength of hydrogen bonds involving either sulfur or oxygen as acceptor,^{1,3} the stabilization energy associated with the N–H···O network was, however, expected to be considerably greater than what was obtained for the equivalent N–H···S interactions. The calculated trends, especially at the MP2 level, do not confirm this expectation. Calculations carried out on the model systems NH₃···(XS–C₂H₄) and (NH₃)₂···(XS–C₂H₄) with X = S or O were then carried out to obtain more detailed information concerning the mechanism and the relative strengths of the H···X interaction in disulfide or sulfoxide complexes.

(31) (a) Stewart, R. F.; Davidson, E. R.; Simpson, W. T. *J. Chem. Phys.* **1965**, *42*, 3175. (b) Allen, F. H. *Acta Crystallogr. B* **1986**, *42*, 515.

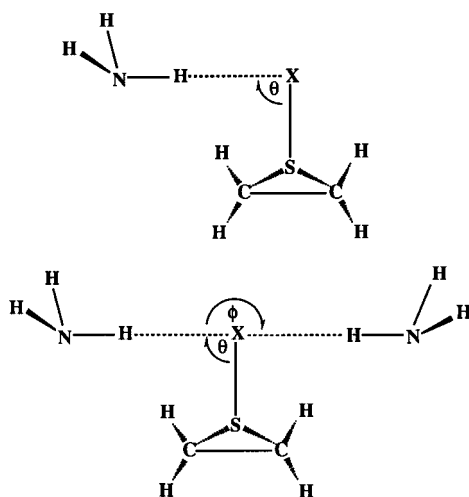
(32) The average value of the observed “heavy-atom to heavy-atom” distances, N···S, is in much better agreement with the calculations. The six N···S distances are between 3.12 and 3.40 Å (average, 3.26 Å), to be compared with computed values of 3.228–3.233 Å.

(33) The topology of this transformation is reminiscent of the new form of isomerism recently characterized by Cotton et al in two complexes with tetrahedral [M₄O]⁶⁺ core (M = Mn, Fe) and C₃ symmetry. See: Cotton, F. A.; Daniels, L. M.; Jordan, G. T., IV; Murillo, C. A.; Pascual, I. *Inorg. Chim. Acta* **2000**, *297*, 6.

(34) Pyykkö, P. *Chem. Rev.* **1997**, *97*, 597.

(35) Wesolowski, T. A.; Ellinger, Y.; Weber, J. *J. Chem. Phys.* **1998**, *108*, 6078.

Scheme 1



5. Models for the Hydrogen Bond in Disulfide and Sulfoxide Complexes

Models had to be designed to explore in more detail the approach of one or two N–H bond(s) to coordinated S–X moieties (X = S, O). They were expected to fulfill the following criteria: (i) reproduce the electronic configuration, the orbital ordering, and as much as possible, the charge distribution of the (S–X)^{2–} ligands in the (TACN)₂Fe₂(SX)₃ complexes, (ii) be obtained by grafting the S–X moiety on a molecular support as innocent as possible with respect to the approach of the NH₃ species, and (iii) remain as small as possible to allow a large number of structures to be optimized in a reasonable amount of computer time. The models eventually selected were NH₃, C₂H₄SX and (NH₃)₂, C₂H₄SX (Scheme 1).

In its equilibrium conformation optimized from DFT calculations, C₂H₄S₂ adequately reproduces the pyramidity at the proximal sulfur (267°) and the overall negative charge of the S₂ fragment, concentrated at the terminal sulfur atom. This negative charge is –0.40e (DFT) in the model, compared to –0.57e for **1**. The S–S bond is shorter by about 0.1 Å. Extended Hückel calculations confirm that the interactions between formally charged (C₂H₄)²⁺ and (S₂)^{2–} conveniently mimics the donation to the di-iron fragment in **1**. The difference in the calculated point charge of the terminal sulfur, however, suggests that the energetics of hydrogen bonding could be underestimated with respect to the real complex. The formation of one N–H···S hydrogen bond was modeled by the lateral approach of one NH₃ molecule.³⁶ One N–H bond and the terminal sulfur were constrained to lie on the same axis assumed first perpendicular to the S–S bond and approximately parallel to C–C ($\theta = \text{H–S–S} = 90^\circ$; $\phi = \text{H–S–H} = 180^\circ$). A “linear transit” was carried out using the DFT formalism by varying the H···S_{term} distance between 5.0 and 2.2 Å with the above constraints and reoptimizing all other parameters at every point (see Supporting Information). Then, the symmetric approach of two NH₃ molecules (Scheme 1) was carried out along the same guidelines. The geometries optimized at each point of the linear transit were then used to derive the potential energy curves at the ab initio

(36) Another possibility for modelling the acidic moiety would have been to consider an ammonium ion NH₄⁺. This model would obviously yield a much stronger interaction with very short S···H distances. The existence of a charge transfer of ~0.2e from each macrocycle to the core and the higher negative charge of the terminal sulfur in **1** suggest that the electrostatic interactions in the complex should be somewhat stronger than those in the neutral model. However, the choice of a positively charged model would grossly exaggerate those interactions.

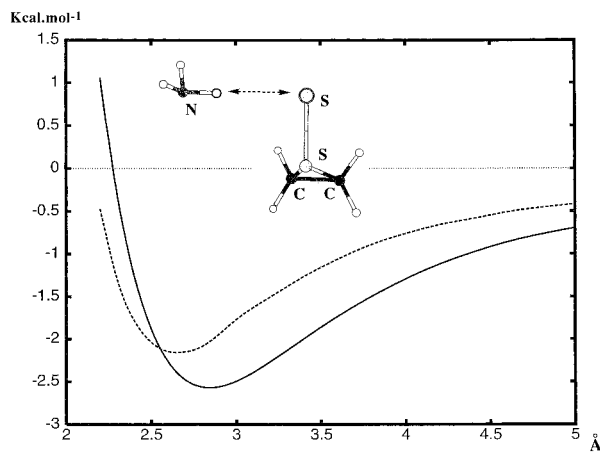


Figure 3. C₂H₄SS···HNH₂ model system: diagram of the N–H···S interaction energy as a function of the H···S distance (Å). Broken line, gradient-corrected DFT, BP86 functional. Solid line: ab initio MP2.

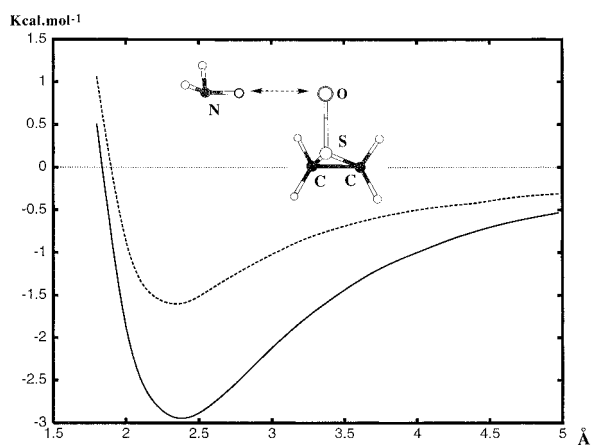


Figure 4. C₂H₄SO···HNH₂ model system: diagram of the N–H···O interaction energy as in Figure 3.

MP2 level. The potential energy curves associated with the approach of one NH₃ molecule to C₂H₄S₂ and calculated at the DFT and ab initio MP2 levels are displayed in Figure 3. Similar curves are displayed in Figure 4 for C₂H₄SO.

Calculations show that the energies involved in the lateral approach of two NH₃ molecules coming from opposite directions are fully additive: either with DFT or with MP2, the stabilization energies calculated with 2NH₃ at any distance are practically twice the energies obtained with a single NH₃ molecule. The model considered for the approach of two NH₃ molecules ($\theta = 90.0^\circ$; $\phi = 180.0^\circ$) does not exactly lead to the environment of the terminal sulfur observed in complex **1** ($\theta = 76.7^\circ$; $\phi = 117.7^\circ$). However, single point calculations performed at $d(\text{H}\cdots\text{S}) = 2.65 \text{ \AA}$, $\theta = 90.0^\circ$, and $\phi = 120.0^\circ$ showed that additivity is conserved assuming the considered parameters.

The minimum of the DFT potential energy curve for the disulfide/ammoniac model is obtained at $d_{\text{H}\cdots\text{S}} = 2.65 \text{ \AA}$ and corresponds to a stabilization energy of 2.04 kcal·mol^{–1} with respect to the complete dissociation of one NH₃ molecule. BSSE-corrected MP2 calculations yield the minimum at a still larger distance ($d_{\text{H}\cdots\text{S}} = 2.84 \text{ \AA}$) although the stabilization energy is somewhat greater at 2.56 kcal·mol^{–1} (Figure 3). The H···S distance at equilibrium is in keeping with the hydrogen bond length obtained by Vibok and Mayer from BSSE-free SCF calculations on the NH₃···SH₂ model (2.9 Å).³ However, the stabilization energy obtained with the present model is consistently higher than that obtained with NH₃···SH₂ (1.4 kcal·mol^{–1}).

This difference should be attributed to the more favorable electrostatic environment provided by the disulfide moiety, since the point charge assigned to sulfur in H₂S is expected to be positive.⁵ The present results suggest, however, that the strength of the interactions involved in complex **1** could still be more important. A first hint is given by the gap between the H···S distances found in **1** (2.32 Å in the optimized geometry, about 2.4 Å (av) in the observed structure, after correction of the hydrogen positions) and the much longer equilibrium distances optimized in the model. Then, the energy difference computed between conformations **1** and **2** (1.7 kcal·mol⁻¹ per hydrogen bond with DFT) is assigned to a stretching of the H···S distance by 0.35 Å only. The curves of Figure 3 show that the H···S interaction is extremely far-reaching: the interaction energy is divided by two when the distance is being stretched by 1.2 Å from the minimum. It would probably be insane to extrapolate from such data the value of the stabilization energy associated with one N–H···S bond in **1**. Although the model adequately mimics the orbital interactions in the Fe₂S₆ core and the polarization of one disulfide fragment, it accounts neither for the increased nucleophilicity of the complex core caused by the vicinity of three negatively charged S₂ ligands nor for the enhanced electrostatic attraction implied by the positive charge of the TACN macrocycles. Both factors will obviously contribute to increase the strength of the N–H···S interactions in the complex. Those interactions could therefore represent the key to the stabilization of three μ - η^1 -S₂ ligands.³⁷

The potential curves of Figure 4 are relative to the lateral approach ($\theta = 90^\circ$) of one NH₃ to the oxygen atom of a C₂H₄-SO molecule. The interaction with two NH₃ molecules confirms that the additivity of the interactions is complete as for the C₂H₄S₂ model. In contradiction with the well-documented trend of hydrogen bonds involving first-row elements to be more energetic than equivalent interactions with second-row elements,^{1–6} the stabilization energy at the minimum was calculated to be 1.59 kcal·mol⁻¹ only at the DFT level. This result appears surprising, even though the interaction energy calculated at the MP2 level (2.98 kcal·mol⁻¹) is slightly larger than that for the disulfide model. Since the optimal directionality of hydrogen bonds to sulfur and to oxygen has been predicted⁵ and observed^{5,6} to be different, i.e., more “perpendicular” in complexes involving sulfur bases, we have considered in our NH₃···XSC₂H₄ models the evolution of the H bond energetics as a function of the H···X–S (θ) angle. The results are displayed in Figure 5. They confirm that the S–S and the S–O fragments behave differently as basic moieties in a N–H···X–S interaction. In the model describing an interaction with disulfide, q_{\max} , the HXS angle corresponding to the most favorable interaction is clearly less than 90° (86° with DFT; 78° with MP2), and the stabilization involved in an approach collinear to the S–S axis is close to zero at the DFT level. It should be noted that the H···S–S angle calculated in complex **1** is 76.7° (Table 1), indicating that the steric conditions in the complex are optimal for the interaction. For a sulfoxide moiety, q_{\max} is shifted toward higher angular values (116° with DFT, 112° with MP2). The stabilization energy obtained with DFT peaks at 2.15 kcal·mol⁻¹ in that direction and remains relatively important (1.49 kcal·mol⁻¹)

(37) The only previous example of a complex with the μ - η^1 -S₂ ligand has been observed in the Cr₂S₅ core of the Cp*₂Cr₂(μ -S)(μ - ν^1 -S₂)(μ - η^2 - η^2 -S₂). See: Brunner, H.; Wachter, J.; Guggolz, E.; Ziegler, M. L. *J. Am. Chem. Soc.* **1982**, *104*, 1765. For reviews on sulfur-rich metal complexes, see: Müller, A.; Jaegermann, W.; Enemark, J. H. *Coord. Chem. Rev.* **1982**, *46*, 245. Wachter, J. *Angew. Chem., Int. Ed. Engl.* **1989**, *28*, 1613. For more recent work on metal–sulfur complexes, see: Inomata, S.; Hiyama, K.; Tobita, H.; Ogino, H. *Inorg. Chem.* **1994**, *33*, 5337. Allshouse, J.; Kaul, B. B.; Rakowski DuBois, M. *Organometallics* **1994**, *13*, 28.

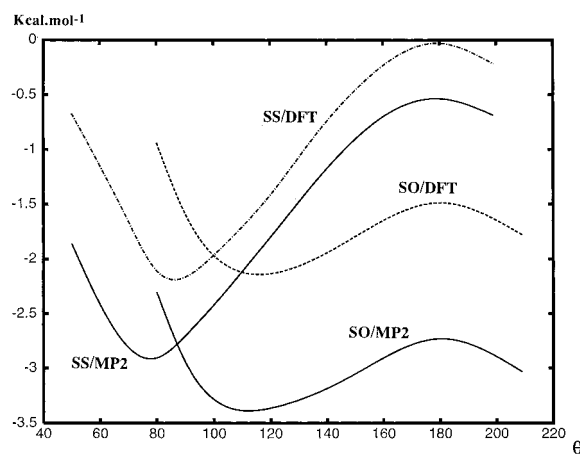


Figure 5. C₂H₄SX···HNH₂ model systems (X = S, O): diagram of the N–H···X interaction energy as a function of the H···X–S angle θ . Broken lines: gradient-corrected DFT, BP86 functional. Solid lines: ab initio MP2.

at 180°. The optimal H···O–S interaction energy obtained with MP2 (3.37 kcal·mol⁻¹) is larger than that obtained with the disulfide model (2.93 kcal·mol⁻¹) and the interaction energy at $\theta = 180^\circ$ remains quite large (Figure 5). If we compare now the energy of the hydrogen bonds at fixed θ values, the H···S–S interaction appears stronger than the H···O–S one at all levels of calculation as soon as θ becomes lower than 87° (Figure 5). Those trends can explain the rather surprising results calculated for the hypothetical sulfoxide complexes (μ -SO)₃(Fe-TACN)₂ assuming conformations **1** and **2** (Table 1). The optimal H···X–S angle has been increased by about 12° with respect to the disulfide complex, but due to the steric constraints, the equilibrium values of $\sim 89^\circ$ are not sufficient to maximize the strength of the hydrogen bonds. As a consequence, the global stabilization of form **1** with respect to form **2** in the sulfoxide complex barely exceeds that of disulfide at the DFT level, and is strikingly lower with MP2 (Table 1).

Similar trends concerning the directionality of hydrogen bonds to sulfur and oxygen were noted and analyzed by Platts et al.⁵ on the complexes of HF with H₂O, H₂S, H₂CO, and H₂CS. The analysis proposed by Platts to explain this different behavior was based upon a decomposition of the H···X electrostatic interaction energy into contributions from atomic multipoles. The critical differences between the H···S and the H···O interactions were (i) the opposite signs of the monopole–monopole (charge–charge) interactions, the net charge assigned to sulfur being positive in H₂S and H₂CS, and (ii) the important stabilizing contribution from the interaction between the charge on H and the quadrupole on S. In the present disulfide and sulfoxide molecules the net charge of the terminal atom is strongly negative for either X = S or O and the charge–charge term is therefore expected to give the most important contribution to the stabilization energy of both types of hydrogen-bonded complexes. The anisotropy of the charge distribution, which accounts for the contribution of the multipoles, will, however, continue to represent an important factor conditioning the directionality of the hydrogen bonds. The effect of this anisotropy in the vicinity of the terminal X atoms of the models will be discussed elsewhere in relation to the calculated distribution of the molecular electrostatic potentials.³⁸

6. Summary and Conclusions

The recently synthesized complex (μ - η^1 -S₂)₃(Fe-TACN)₂ (TACN = triazacyclononane) is quite unusual in several

(38) Rohmer, M.-M.; Bénard, M. Manuscript in preparation.

aspects: the occurrence of a M_2S_6 core is unprecedented, and only one example is known of a $\mu-\eta^1-S_2$ ligand.³⁶ A theoretical investigation of the electronic and structural singularities of this complex has been reported, with particular emphasis on the energetics of the network of intramolecular $H\cdots S$ bonds revealed by the crystallographic analysis. An extended Hückel analysis of the bonding between the $Fe(TACN)$ dimer and the three persulfide ligands accounts for the diamagnetism of the complex, the presence of a metal–metal single bond, and the nucleophilicity of the terminal S atoms. The Mulliken point charge and fragment charge analysis confirms that the terminal sulfurs have a strong negative charge (ca. $-0.6e$) and reveals that a significant charge transfer ($\sim 0.2e$) occurs from each macrocycle to the Fe_2S_6 core. Then, geometry optimizations have been carried out by means of the Density Functional Theory (DFT) on two configurations of the $(\mu-\eta^1-S_2)_3(Fe-TACN)_2$ complex which only differ in the strength of the $N-H\cdots S$ bond network. The experimental conformation **1**, characterized by six “strong” $N-H\cdots S$ bonds ($d_{H\cdots S} = 2.31$ Å), is more stable by 10.0 kcal·mol⁻¹ than the hypothetical structure **2** with “weak” hydrogen bonds ($d_{H\cdots S} = 2.65$ Å). Replacing persulfide by sulfoxide ligands leads to a similar energy difference (11.4 kcal·mol⁻¹), despite the well-documented tendency to obtain stronger H bonds with oxygen than with sulfur. Those results are rationalized by means of a systematic investigation, at the DFT and MP2 levels, of the $N-H\cdots S$ and $N-H\cdots O$ interactions in the model systems $C_2H_4(SX)$, NH_3 ($X = S, O$). The strength of the $N-H\cdots X$ interaction is shown to be highly dependent on the directionality of the hydrogen bond characterized by the angle $\theta = H-X-S$. For $X = S$, the optimal interaction is obtained for $\theta \sim 80^\circ$, which almost exactly reproduces the angular parameter optimized in **1** (76.7°). For $X = O$, the interaction is most favorable for higher values of θ ($\sim 115^\circ$) which cannot be obtained in the hypothetical compound $(\mu-\eta^1-SO)_3(Fe-TACN)_2$ because of structural constraints. Important differences are obtained between the equilibrium $H\cdots X$ distances in

conformation **1** of both complexes and in the corresponding models. The distance, optimized at the DFT level, is shorter in the complexes by 0.33 Å for $X = S$ and by 0.20 Å for $X = O$. This difference is assigned to an enhanced electrostatic attraction in the complexes, originating in (i) a greater negative charge on the terminal atoms of the complexes, (ii) a deeper electrostatic potential in the complex core due to the accumulation of three nucleophilic SX ligands, and (iii) the effect of charge transfer inducing an electric dipole between the $(SX)_3$ core and each macrocycle. Finally, varying the $H\cdots X$ distance in the models shows that those interactions are extremely far-reaching. The $N-H\cdots S$ interaction energy computed with DFT still reaches 1.2 kcal·mol⁻¹ at $d_{H\cdots S} = 3.5$ Å and approaches 0.5 kcal·mol⁻¹ at 5 Å. The energy difference between conformations **1** and **2** then accounts for a small fraction only of the global stabilization due to the hydrogen bond network, which could hence represent the key to the stabilization of the Fe_2S_6 core.

Acknowledgment. Calculations were shared between the workstations of the Institut du Développement et des Ressources en Informatique Scientifique (IDRIS, Orsay, France), those of the Centre Universitaire et Régional de Ressources en Informatique (CURRI, Université Louis Pasteur, Strasbourg, France), and those of the Laboratoire de Chimie Quantique. We are grateful to Dr. Lilyane Padel and Sylvie Fersing for their kind and patient assistance.

Supporting Information Available: A full description of the geometries optimized for complexes $(TACN)_2Fe_2(SX)_3$ ($X = S, O$) in conformations **1** and **2** (Cartesian coordinates in Å) and similar information for the various investigated conformations of the model systems $C_2H_4SX\cdots HNH_2$ as well as bonding energies (DFT) and total energies (MP2) associated with every conformation (PDF). This material is available free of charge via the Internet at <http://pubs.acs.org>.

JA0011717